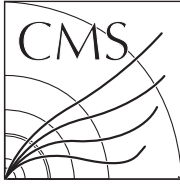
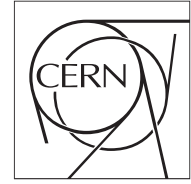


2

**The Compact Muon Solenoid Experiment**

CMS Note

Mailing address: CMS CERN, CH-1211 GENEVA 23, Switzerland



3

4

August 28, 2009

5

Efficiency Measurements in the CSC Muon End Cap System

6

7

Stoyan Stoynev and Michael Schmitt
Northwestern University

8

9

Abstract

10

The CMS Cathode Strip Chambers (CSC) provide tracking for muons in the endcaps. They are designed to have a very high efficiency for triggering and for tracking. An offline analysis package, *CSCEfficiency*, allows the measurement of several efficiencies in a manner that can be applied to both real and simulated data. CSC efficiencies have been measured with cosmic ray data taken in 2008, and in general the performance of the CSC's is excellent. A feature of the trigger peculiar to cosmic rays sometimes caused the track from a single cosmic ray event to be split between two events; changes to trigger timing have been made for the sake of cosmic ray running in 2009.

1 Introduction

The Cathode Strip Chambers (CSC) are part of the CMS muon endcap system and are required to be above 99% efficient per chamber for finding segments of muon tracks. This is important for the accurate assignment of the bunch crossing number and for an accurate reconstruction of muon trajectories. Needless to say, various physics analyses (for example $H \rightarrow ZZ^* \rightarrow 4\mu$) will rely on a highly efficient muon system. A cross-sectional view of the CMS detector showing the CSC's is given in Fig. 1. Detailed descriptions of the CSC subdetector system can be found in Ref. [1].

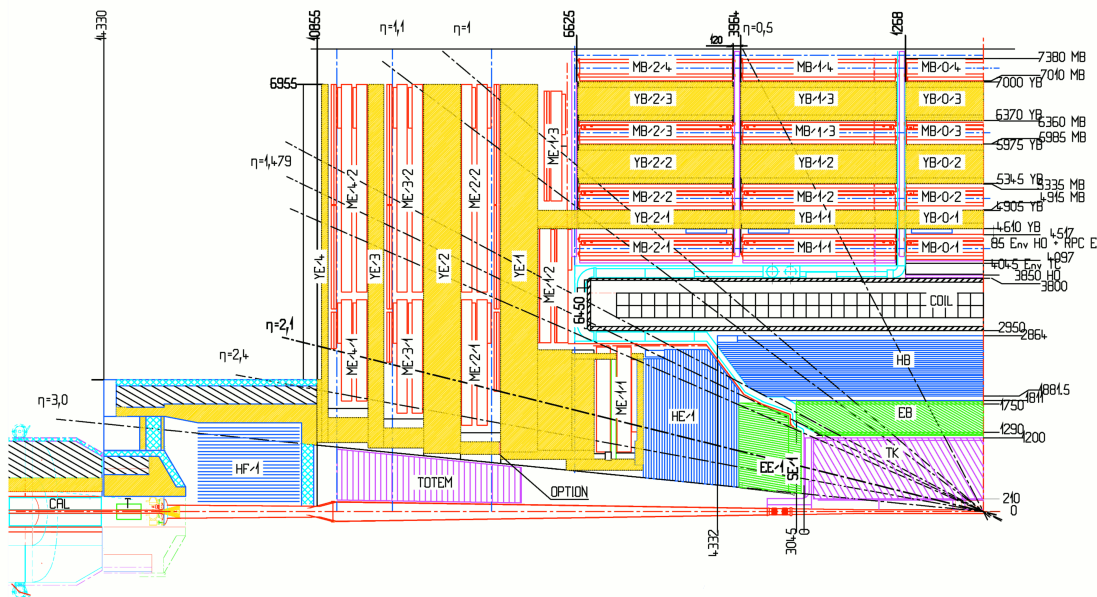


Figure 1: cross-sectional view of the CMS detector. Four CSC stations can be identified as the vertical red box on the left half of the figure. Note that the $ME_{\pm 4/2}$ chambers have not yet been constructed, being part of the future muon upgrade program. The iron absorber is shown in yellow.

An offline analysis package called *CSCEfficiency* has been developed to provide carefully controlled and unbiased measurements of the CSC efficiencies. As explained in the next section, several interdependent efficiencies can be defined. The methods we have developed are applicable to real data and do not rely on Monte Carlo truth information. The main idea is to establish that a muon did pass through a given chamber, and then check whether the expected signals were recorded.

The *CSCEfficiency* package was used to measure efficiencies using the CRAFT data sample. "CRAFT" stands for *Cosmic Run At Four Tesla* and refers to a large data sample logged in Fall 2008. Essentially all of the CMS detector was operating correctly, allowing the collection of about 300 million cosmic ray triggers over a four week period. Only a small fraction of these triggers are useful for CSC efficiency measurements; nonetheless, good results have been obtained as reported in the later sections of this report.

2 Methodology

Measuring absolute efficiencies from real data requires some care, both in the definitions of “efficiency” (what is the denominator?) and in defining and validating the methods used for measuring those efficiencies. A general discussion of the problem of defining and obtaining absolute efficiency comes first, followed by certain relevant technical specifications related to the package itself.

Raw data recorded from the detector are unpacked into digis. There are digi collections for the strip signals, the wire signals, and the local charged track information, among others. The information stored in the digis is processed to produce a collection of rechits with measured x and y coordinates at a known z coordinate. The rechits reconstructed in a given chamber are used to form a straight-line segment, which is fit to provide a measure of the muon track in the chamber. These segments are used to seed the reconstruction of stand-alone muons [2]. The goal is to measure the *absolute* efficiency of each step (local charged track trigger, presence of the signal in the digis, reconstruction of rechits, and finally segments) in order to identify which step, if any, introduces an inefficiency. When computing the efficiency of each step, the method described here uses the same denominator for all steps, as described in detail below.

2.1 Overview of Efficiencies to be Measured

The readout of a cathode strip chamber is triggered by the presence of Anode and Cathode Local Charged Track patterns, referred to as ALCT and CLCT, respectively. They are defined in the trigger logic [1, 3]. There is also a correlated LCT based on the coincidence of an ALCT and CLCT. We need to measure the efficiency for producing an ALCT, CLCT and correlated LCT given a track passing through the chamber. Clearly this efficiency is dependent on the efficiencies of the six individual chamber layers. Currently, the firmware requires at least four layers for forming an LCT.

To check the quality of the data to be used for track reconstruction, one should start with the efficiency of having strip and wire group signals. Strip and wire group efficiencies are defined for every layer, or possibly sub-regions within the layer. They could even be defined for a specific strip or wire group when one studies the efficiency as a function of the position. In this way, dead or problematic regions within a layer can be identified.

Rechits are constructed with the information extracted from the strips and wire groups. These represent the measurement of the intersection point between the track and a CSC layer. The rehit efficiency amounts to the probability to find a rehit in a layer given that a muon passed through it, and depends on how well the CSC functions, on the design of the chamber and on the offline reconstruction algorithm.

The last level in the CSC local reconstruction is the segment building. A segment is constructed from the rechits in different layers. Only one rehit is used from any given layer, and a minimum number of three rechits is required. The efficiency for building segments depends on both the rehit quality and the segment reconstruction algorithm. For a better understanding of the performance of the segment reconstruction algorithm, one can define a so-called “attachment efficiency.” This is the probability that a rehit in a given layer is attached to the segment. In this context, the absolute efficiency is not the most important issue; rather, one is interested in the way the segment builder efficiency may vary with layer number, angle, *etc.* The attachment and segment efficiencies depend on the segment finder

75 algorithm through several parameters, such as the allowed number of rechits common to
76 two segments, the minimum number of rechits in a segment, the allowed ranges of angles or
77 distances used in the reconstruction, *etc.*

78 2.2 Defining Good Regions of a Chamber

79 Usually one needs to investigate the “intrinsic” properties of a chamber or layer, so one needs
80 to define “good regions” that are governed predominantly by intrinsic processes and not by,
81 for example, geometric dead regions which reduce the value of the efficiency without telling
82 us whether the chamber is working well. There is little point in taking into account regions
83 which cannot produce a hit when measuring efficiencies if the purpose is to check that a
84 chamber and offline reconstruction software are functioning well. In this sense, defining
85 the good region of a chamber is the same as identifying a region which is fully sensitive to
86 muons, at least at the design level.

87 Dead regions in the CSC’s are defined primarily by the boundaries between high voltage
88 segments. In certain cases it might be interesting to further sub-divide the HV segment into
89 zones defined by CFEB (Cathode Front-End Boards) boundaries, but in general this will not
90 be done. We have checked that there is no anomalous behavior at the CFEB boundaries.

91 The definition of “good regions” in the CSC’s depends to some extent on the types of events
92 available for study. At present, only muons from cosmic rays are available, and a large
93 sample of high-momentum muons passing nearly perpendicular to the chambers is very
94 difficult to collect. Consequently, multiple scattering and magnetic field uncertainties pose
95 significant issues to be considered carefully when defining good regions in the CSC’s¹.

96 Most cosmic rays above ground have an energy of at most a few GeV [5]. In the underground
97 cavern at P5, the energies are shifted to somewhat higher values. Muons passing through
98 three consecutive CSC stations must have energies of at least a few GeV². Even with the
99 effective minimum-momentum cut imposed by the trigger, many muons have an energy of
100 only a couple of GeV, and multiple scattering in the yokes can displace the muon’s trajectory
101 by several centimeters with respect to the expected position.

102 Fig. 2 shows distributions of the difference between the measured position of a segment
103 in the probe chamber and the predicted position, obtained by propagating the muon track
104 from another station to the probe chamber. In this figure, X and Y refer to local coordinates.
105 Nearly all of the tracks fall within 10 cm of the predicted position.

106 Fig. 3 shows the distribution of measured local y coordinates in a chamber. The right-hand
107 plot shows a close-up of the end of the chamber at large y ; the nominal end of the sensitive
108 region is 94 cm. The distribution rises linearly from $y < 0$ to $y > 0$ due to the trapezoidal
109 shape of the CSC’s. The fall off of the distribution above 85 cm justifies the 10 cm criteria,
110 which amounts to $y < 84$ cm in this case.

111 2.3 General Techniques

112 For efficiency measurements, we need a well-defined muon track which is independent of
113 the measurements in the chamber under investigation. In collision data the best choice is
114 a muon reconstructed simply as a track in the Si tracker, which can be propagated to the

¹Useful calculations of multiple scattering in the CSC subdetector can be found in Ref. [4]

²A typical thickness for the iron yokes is 60 cm (or $\sim 34X_0$) which means a minimum-ionizing muon deposits a bit less than 1 GeV in each yoke depending on the penetration angle

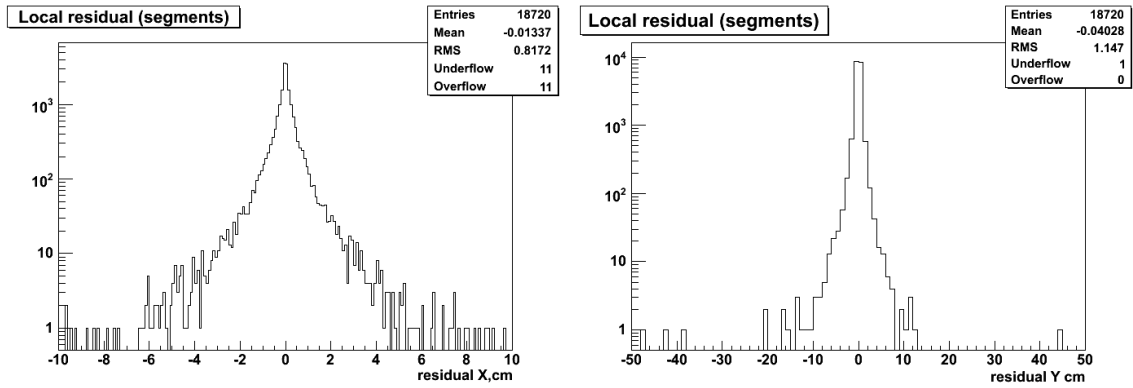


Figure 2: differences between the predicted positions of a segment and the position of the reconstructed segment in the probe chamber. ΔX is on the left, and ΔY is on the right, where X and Y are local coordinates. X is measured primarily by the strips, and Y is measured by the wires

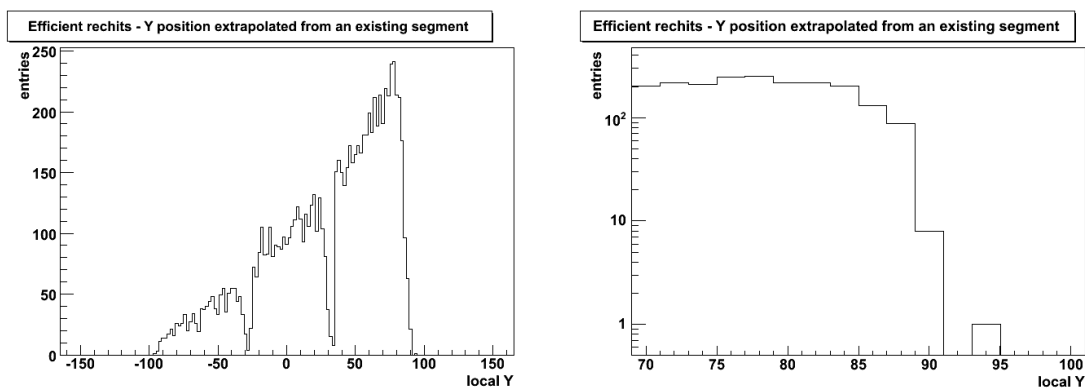


Figure 3: distribution of measured local y coordinates in chambers from rings ME2/1. (LEFT:) full range in y (RIGHT:) close-up near the end of the sensitive range. The nominal end of the sensitive range is $y = 94$ cm

1	Trigger bit <code>HLT_L1MuOpen</code> is set.
2	No more than one muon track from the <code>cosmicMuons</code> collection per hemisphere
3	$\chi^2/ndf < 3$ for the muon track fit
4	At least ten hits on the muon track
5	At least one CSC segment present in the detector
6	momentum of the track: $25 \text{ GeV} < P < 100 \text{ GeV}$
7	stable magnetic field at 3.8 T, and $\sigma_{P_t}/P_t < 0.5$
8	the track should pass at least 10 cm away from edges and dead regions of a chamber
9	the chamber should not be at the end point of the track

Table 1: criteria applied to select a sample of good “probe” tracks from the CRAFT data.

115 CSC’s as desired. High energy muons will not be rare and so multiple scattering effects
 116 will not be an important issue. In cosmic ray data, however, high energy muons passing
 117 through the tracker and the endcaps are rare, and in practice there are not enough of them.
 118 Instead, we use muon tracks reconstructed in several CSC’s without any information from
 119 the Si tracker – these are the “stand-alone” muons. The number of useful stand-alone muons
 120 is adequate for the present purposes, thanks to the redundancy of the muon endcap system.
 121 There are some additional problems, however: the independence of the reconstruction of the
 122 stand-alone muon track of the probe chamber is less evident, and the momentum precision
 123 is worse than that of a track in the Si tracker. To minimize the impact of these difficulties, a
 124 chamber is probed only if it lies between the endpoints of the track ³. Consequently, at least
 125 two independent measurements of the muon track are needed, and only interpolation and
 126 not extrapolation to the probe chamber is used.

127 It proved difficult to define a subset of cosmic ray muons which could be used for accu-
 128 rate efficiency measurements. Through prolonged studies of real and simulated cosmic ray
 129 events, we developed some criteria to select “good” tracks for the denominator of all effi-
 130 ciency calculations. Only one stand-alone muon track is allowed in an endcap. This track
 131 has to have at least a minimum number of hits, and to be reconstructed well, as indicated
 132 by the χ^2 and the relative error on the momentum. A good track satisfying these require-
 133 ments is propagated ⁴ to a designated ring of CSC chambers to ascertain which chamber is
 134 the probe chamber. If the interpolated point lies close to the edges of the chamber or dead
 135 regions defined by HV segment boundaries, then the chamber is skipped. The criterion for
 136 “close” depends on the typical muon momentum and its uncertainty, and may be different
 137 for samples of cosmic ray muons and muons produced in collisions. We need to ensure that
 138 only a very small number of tracks passing outside good regions are used in the efficiency
 139 calculations, and consequently we have to sacrifice a significant number of otherwise good
 140 tracks.

141 Suitable tracks are selected using the criteria listed in Table 1. These criteria are appropri-
 142 ate for cosmic ray tracks; others will be needed once collision data are available. The tracks
 143 which pass all of these criteria are the probe tracks – their number appears in the denomina-
 144 tor in the efficiency calculation for all interesting quantities, ranging from LCT’s to segments.

145 2.4 Formal Definitions

146 The efficiencies obtained with the `CSCEfficiency` package are defined as follows.

³also known as the inner and outer “surfaces” of the track

⁴The so-called “stepping helix propagator,” an official tracking tool in CMS, is used.

147 **LCT Efficiencies:** The ALCT and CLCT efficiencies are measured independently. The “probe”
148 or “denominator” is given by all tracks satisfying the criteria in Table 1. For a given chamber,
149 the ALCT and CLCT digis are unpacked to test for the presence of a valid ALCT or CLCT.
150 If they are present anywhere in the chamber, then the trial is a “success” and the chamber is
151 “efficient” for that event.

152 **Strip and Wire Digi Efficiencies:** In principle, the presence of an ALCT and CLCT should
153 trigger the read out of the chamber, and hence, signals on the wires and strips should be
154 present in the raw data, or equivalently, in the strip and wire digis. The efficiency for strip
155 and wire digis are measured independently. The probe is given by a good track passing
156 through the given chamber. There is no requirement that ALCTs and CLCTs be found in
157 that chamber before proceeding to test the strip and wire digis. The chamber is efficient if
158 any wires or strips are present in the chamber - no attempt is made to match the wire group
159 or strip numbers to the position of the probe track. The requirement that there be only one
160 probe track is important in this regard.

161 **Rechit Efficiency:** The efficiency for reconstructing a rechit is measured for each layer in
162 a chamber. The chamber is efficient if the rechits are found in a given layer - there is no
163 requirement on the distance between the rechit and the interpolated point. Also, no qual-
164 ity requirements are placed on the individual rechits as part of the measurement of rechit
165 efficiency.

166 **Segment Efficiency:** It should be possible to build a segment if at least three good rechits are
167 recorded along the muon trajectory. The chamber is efficient if a segment has been recon-
168 structed. No matching criteria have been applied (cf. Fig. 2).

169 **Attachment Efficiency:** If a segment has been reconstructed, it will usually have six hits -
170 one from each layer. One can measure the rate at which each layer fails to have a rechit on
171 the segment when a rechit is present in the layer. This is called the “attachment efficiency.”
172 As noted earlier, the segment builder may remove a rechit which is incompatible with the
173 fitted segment or which has poor quality. One should check whether this probability is the
174 same for all layers.

175 **3 Results from CRAFT**

176 The CRAFT data comprise some 300 million cosmic muon triggers, most of which came
177 from the drift tube barrel detectors. Most of the muons triggered in the endcaps are not
178 useful because their trajectories are steeply inclined or pass through only an edge of one
179 of the endcaps. Only a minute fraction of the recorded cosmic ray muons follow a useful
180 path through the endcaps, and satisfy the nominal geometric requirements for the ALCT
181 and CLCT discussion in Section 3.2 below. About 70% of the CRAFT data survive standard
182 good run requirements, and after imposing the cuts in Table 1, about 120,000 events remain.

183 Events were recorded with a very loose CSC trigger based on the logical “OR” of the trigger
184 signals of all individual chambers. A typical event selected for these efficiency measurements
185 contains three or four CSC’s contributing to a good stand-alone muon track. Since the trigger
186 efficiency is generally high (see below), and a trigger from any one of these chambers sufficed
187 to produce a trigger for read out of CMS, we assume that any trigger bias in the results is
188 negligible.

189 We used CSCEfficiency from offline version CMSSW_2_2_6. The CRAFT data were recon-

190 structured with CMSSW_2_2_0.

191 As emphasized above, the quality of the cosmic ray data is limited for the purposes of mea-
192 suring efficiencies. In order to make reliable measurements, we require that the minimal mo-
193 mentum of the stand-alone muon is 25 GeV. We also require that it pass at least 10 cm away
194 from any edge of the probe chamber, and from the boundaries of HV segments. Chambers in
195 rings $ME\pm 4/1$, $ME\pm 1/1$ and $ME-3/2$ are necessarily at the endpoint of a stand-alone muon
196 track, which precludes any interpolation into chambers in these rings⁵. Data recorded with
197 the endcap RPC's do allow measurements of the efficiencies in $ME+3/2$, however.

198 In 2008, approximately twenty chambers out of 468 were not fully operational. Their per-
199 formance varied through the CRAFT data-taking period. When measuring efficiencies for a
200 ring, we excluded known non-functioning chambers.

201 A sample of simulated cosmic rays events generated and reconstructed with CMSSW_2_2_9
202 was used to validate all analysis methods applied to the CRAFT data. The efficiencies mea-
203 sured with these simulated data were essentially 100%, as expected.

204 3.1 The Problem with Split Events in CRAFT

205 During the course of these efficiency measurements, a very low efficiency around 50% was
206 observed for the CLCT's from chambers in the lower half of the detector ($y_{\text{global}} < 0$). The
207 efficiency on the upper half ($y_{\text{global}} > 0$) was higher, around 90%.

208 The low efficiency eventually was shown to be the consequence of a trigger timing feature.
209 One of the trigger rules allows a second Level-1 Accept signal (L1A) as soon as 3 beam
210 crossings (BX) after the first one. A nearly horizontal cosmic ray muon requires about 2.5 BX
211 to traverse both muon endcaps. It will enter CMS at one end with $y_{\text{global}} > 0$ and exit the
212 other with $y_{\text{global}} < 0$. This kind of event is favored by the directional cuts (Eq. 1) discussed
213 below. Due to the asynchronous nature of cosmic rays, some of these muons will produce
214 two L1A's.

215 The key point is how the CSC information is handled if two L1A's are received for the same
216 muon track. Due to the way timing windows had been set, the ALCT information was sent
217 for both L1A's, while the CLCT was sent only once. Consequently, for two consecutive events
218 that were triggered by the same muon, one would see ALCT's from both endcaps in both
219 events, but CLCT's in one event only. The anode wire and cathode strip raw data might or
220 might not be present in both endcaps in either event. Therefore it was possible to reconstruct
221 rechits in chambers with no apparent CLCT response, thus leading to a low CLCT efficiency.
222 We were able to identify pairs of consecutive events with identical ALCT's. When such pairs
223 were excluded from the efficiency measurements, the CLCT efficiency was found to increase
224 dramatically. An example of a split event (two consecutive muon triggers coming 3 BX apart)
225 is shown in Fig. 4.

226 The CSC commissioning group has addressed the trigger feature in a number of ways. Some
227 of the timing windows have been lengthened. The trigger timing of the upper half of the
228 disks is shifted by 2 BX with respect to the bottom half; in 2008 the shift was only 1 BX.
229 Finally, at least some data will be taken triggering only on the bottom half. The drift tube
230 barrel muon detectors will also trigger in this manner.

⁵On rare exception, a stand-alone muon track will pass through the overlap region of two chambers, allowing the efficiency of one of them to be measured. Also, a very rare event will contain a Si track, allowing measurement of chambers in ME1.

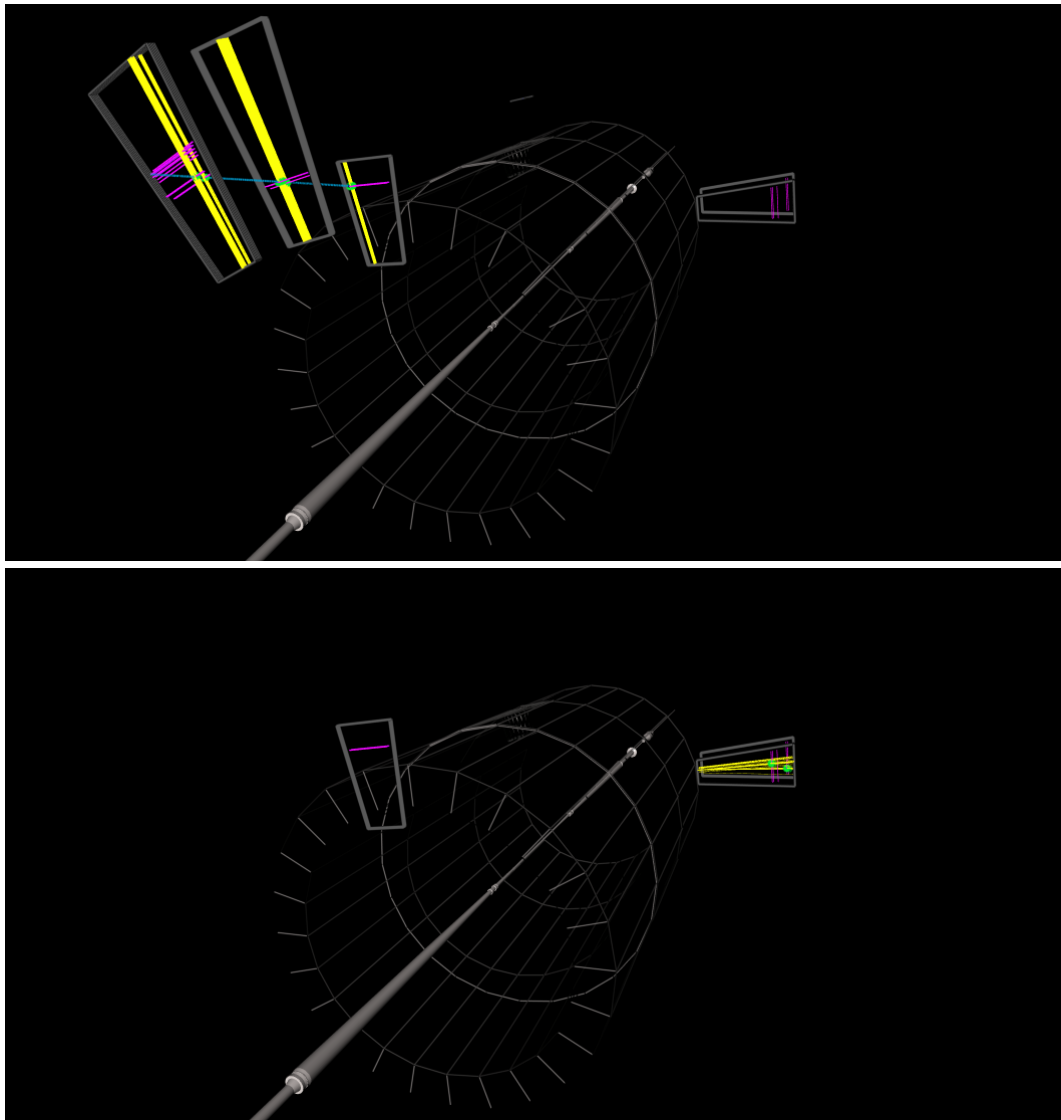


Figure 4: an example of a split event from run 69912. The top event display shows event 1994891, and the bottom, event 1994892. Their triggers are 3 BX apart. It is clear that the signals from one single muon are split between two consecutive events. The second event has no CLCT's while the first has CLCT's from both endcaps.

231 The split event problem leads to low efficiency values for many quantities, since a common
 232 denominator is used for all. A common loss of events would obscure more subtle effects that
 233 may be of interest. For measurements of segment, rechit and digi efficiencies, we impose
 234 an extra requirement of two layers with rechits in the probe chamber. Two hits is below
 235 the threshold for LCT's and for building segments, so it does not bias the values for these
 236 efficiencies. This requirement does remove chambers that are empty due to the split event
 237 problem. It should not be required in the future, when readout windows have been widened
 238 and when collision data are available.

239 3.2 LCT Efficiencies

240 The ALCT wire patterns and the CLCT strip patterns were designed to be efficient only for
 241 muons originating from the interaction point [3]. A representation of the allowed patterns is
 242 given in Fig. 5.

The wire group width varies between 1.5 and 5 cm for different chambers. The distance between layers is 2.54 cm, except for the ME1/1 chambers, for which it is 2.2 cm. The range of track inclination (dy/dz in local coordinates) which should give efficient ALCT response is $-0.59 < dy/dz < 0$ for smaller chambers, and $-1.97 < dy/dz < 0$ for larger chambers. Similarly, for the CLCT response the range is $|dx/dz| < 0.24$ for smaller, and 0.63 for larger chambers. For collision data, the muons should naturally have inclination angles within these ranges. Muons from cosmic rays, however, come in at a wide variety of angles. To suppress the muons which are not likely to fire the ALCT and/or CLCT triggers, we apply cuts on the slopes of the muon tracks interpolated through the chamber:

$$-0.8 < \frac{dy}{dz} < -0.1 \quad \text{and} \quad \left| \frac{dx}{dz} \right| < 0.2. \quad (1)$$

243 One could adjust these ranges for the various rings of chambers, but the impact on the effi-
 244 ciency measurements is negligible. All the efficiencies made with CRAFT data include these
 245 requirements in the event selection ⁶.

246 The variation of the ALCT efficiency as a function of dy/dz is shown in Fig. 6. For this figure,
 247 the cut on dy/dz was not applied, although the cut on dx/dz was applied. Similarly, the
 248 variation of the CLCT efficiency as a function of dx/dz is shown in Fig. 7, with the cut on
 249 dx/dz relaxed and the cut on dy/dz applied. The results shown in these plots are based
 250 on data from chambers 5–13 in ring ME+2/2 which were known to be operating well. In
 251 both figures, clear plateaus can be seen which were fit with level functions to ascertain the
 252 efficiency. Very high values in excess of 0.999 are observed. Earlier measurements carried
 253 out by the Florida group agree with these results [6].

254 Summaries of the average ALCT and CLCT efficiencies in each ring of chambers are pre-
 255 sented in Fig. 8. The full set of cuts (Eq. 1) were applied, and only good working chambers
 256 were used in computing the averages. A different presentation of the data, which allow the
 257 efficiencies of all chambers to be inspected, is given in Appendix B. Fig. 9 gives a closer look
 258 at the ME+2/2 chambers. The impact of the split events is evident.

⁶These requirements were not included in the default `CSCEfficiency` package in `CMSSW_2_2_6`, and were added for these CRAFT measurements.

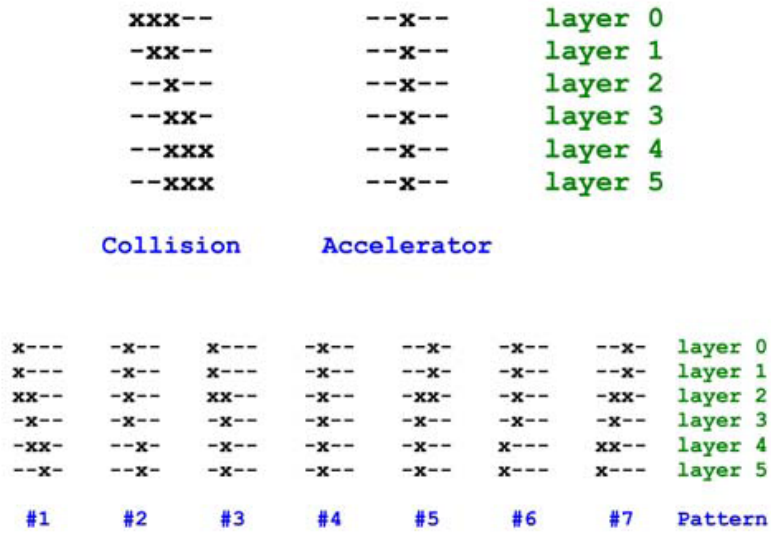


Figure 5: representations of the allowed trigger patterns [3]. The upper diagram shows the wire groups that can produce an ALCT, and the lower diagram shows the strips which can produce a CLCT.

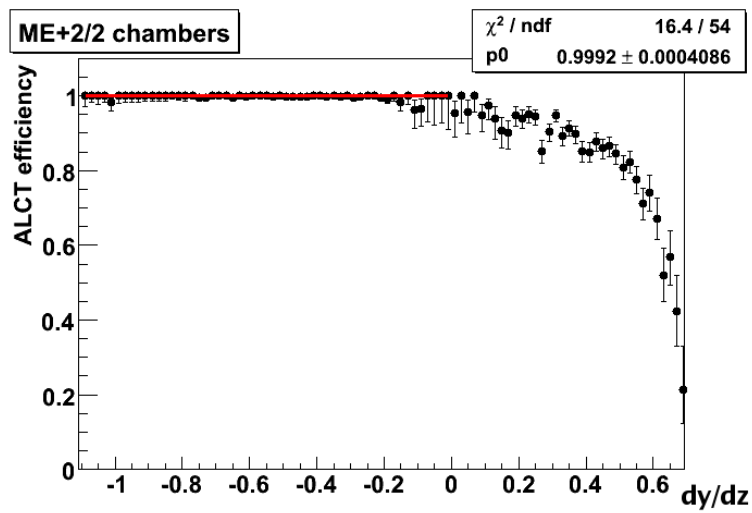


Figure 6: ALCT efficiency as a function of the track inclination, dy/dz in local coordinates

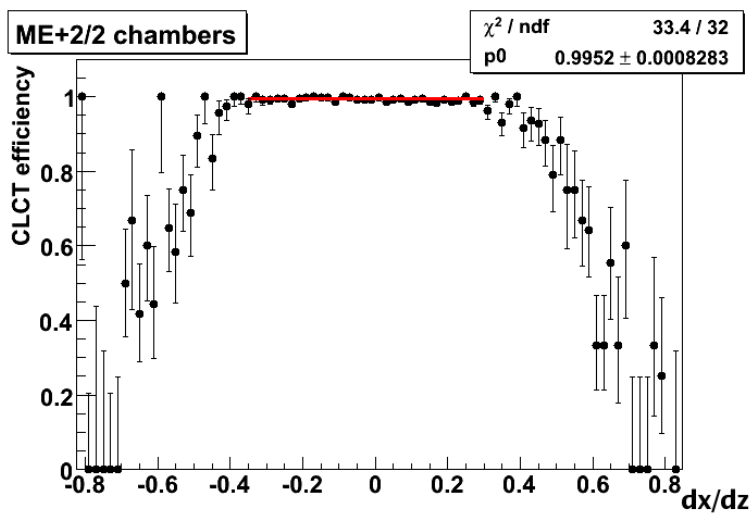


Figure 7: CLCT efficiency as a function of the track inclination, dx/dz in local coordinates

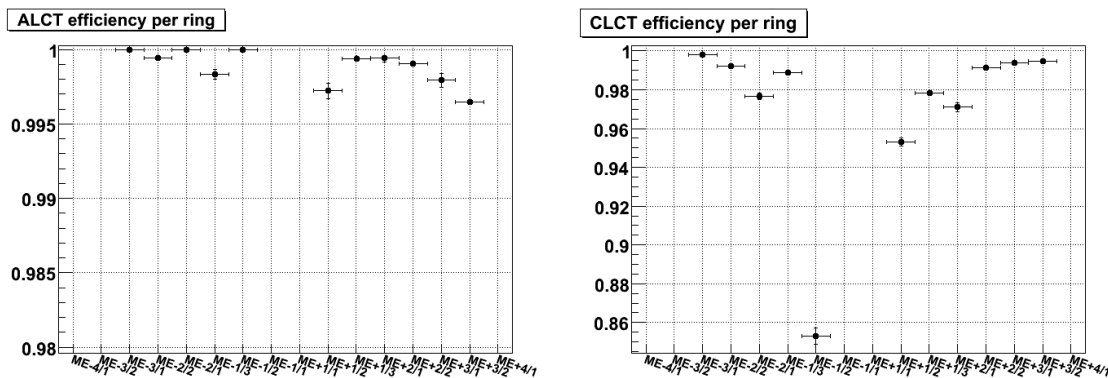


Figure 8: summary of ALCT (left) and CLCT (right) efficiencies for all accessible rings.

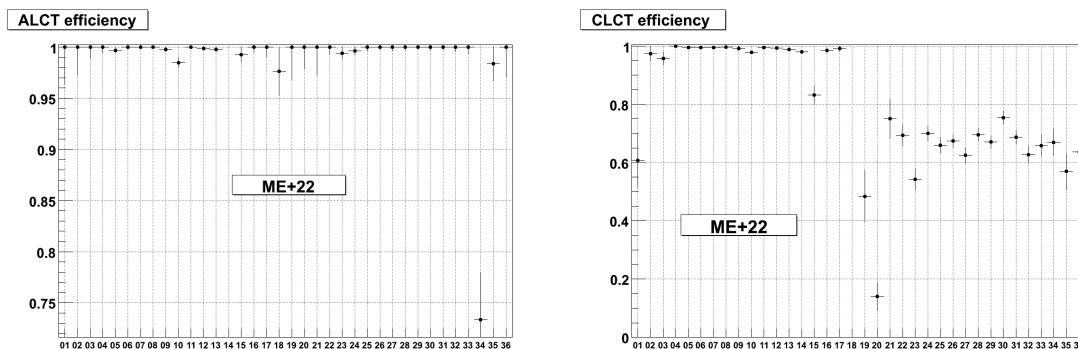


Figure 9: local charged track efficiencies for all chambers in ring ME+2/2. *LEFT*: ALCT's; *RIGHT*: CLCT's

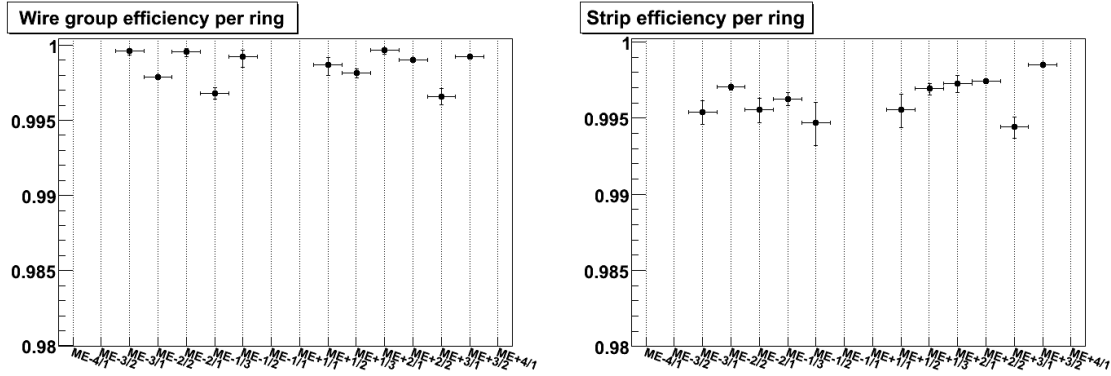


Figure 10: summary of wire group (left) and strip (right) digi efficiencies, over all functioning chambers in a ring. Some rings are inaccessible in this study with CRAFT data.

259 3.3 Strip and Wire Group Efficiencies

The efficiencies of strips, wire groups and rechits are defined naturally per layer. If the layer measurements are independent, then the average efficiency per chamber would be

$$\bar{\epsilon} = \frac{\sum_i \epsilon_i}{L} = \frac{\sum_i n_i}{N \times L} \quad (2)$$

with an estimated uncertainty of

$$\Delta\bar{\epsilon} = \sqrt{\frac{\bar{\epsilon} \times (1 - \bar{\epsilon})}{L \times N}}, \quad (3)$$

260 where $L = 6$ is the number of layers, ϵ_i is the efficiency in layer i ($i = 1, \dots, 6$), n_i is the number
 261 of efficient cases (“successes”) for layer i , and N is the number of probe tracks. In principle,
 262 there might be events with a simultaneous loss of information from all six layers, in which
 263 case Eq. 3 is incorrect. Aside from the problem of split events explained above, there is no
 264 evidence for any such correlated losses.

265 The average wire group and strip digi efficiencies are shown in Fig. 10. An example of “per
 266 layer” efficiency is shown in Fig. 11. Most of the time, the efficiency is very close to 100%,
 267 but in the case of the particular chamber shown, layer 5 has a reduced efficiency, due to some
 268 run during which the HV was off for that layer. Typically, all six layers are highly efficient,
 269 as shown in Fig. 12.

270 3.4 Rechit Efficiency

271 The rechit efficiency will be a convolution of the strip and wire group digi efficiencies. It
 272 might also depend on some of the details of the rechit reconstruction algorithm, especially
 273 as regards quality or other criteria applied to the strip and wire signals.

274 The rechit efficiency for all the rings in the CSC system is shown in Fig. 13. A closer look at
 275 ME+2/2 chambers is given in Fig. 14 which shows that the rechit reconstruction efficiency
 276 is above 99.5%.

277 3.5 Segment Efficiency

278 Ideally, the segment efficiency would be related in a simple and direct way to the rechit
 279 efficiency. The segment reconstruction algorithm, however, also places requirements on the

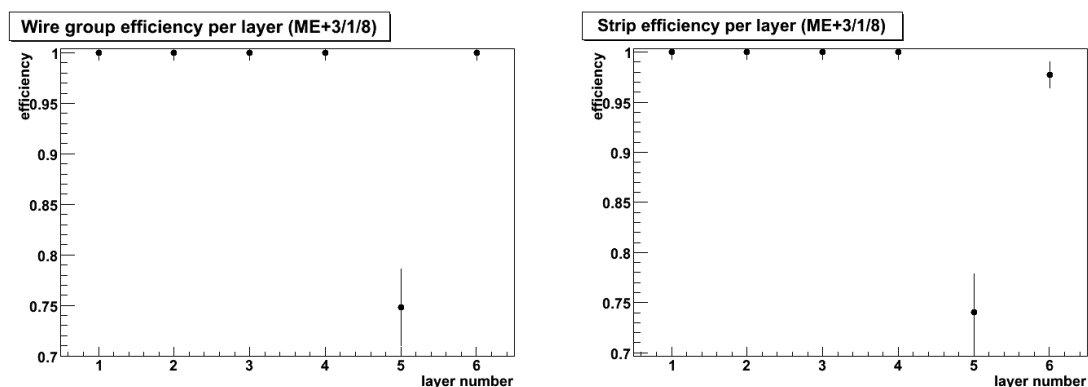


Figure 11: efficiencies for each layer in chamber ME+3/1/18. *LEFT*: wire group efficiency; *RIGHT*: strip efficiency. This chamber was selected since layer 5 has a slightly lower efficiency than usual, due to a temporary high-voltage problem.

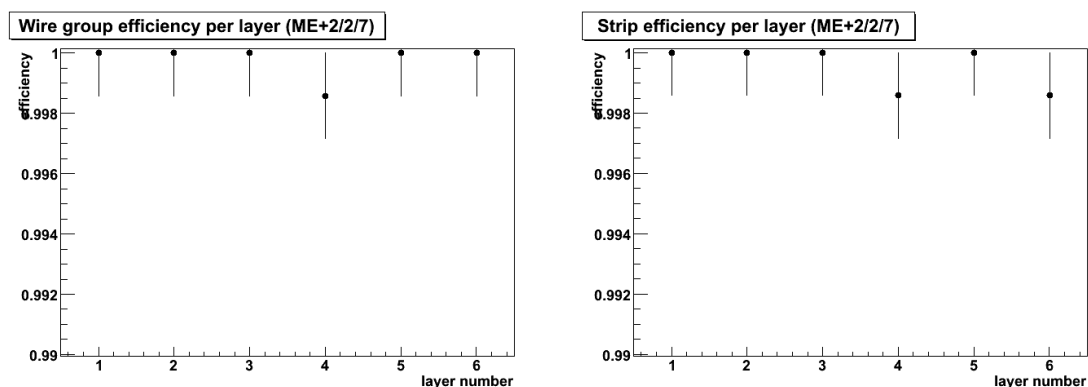


Figure 12: efficiencies for each layer in chamber ME+2/2/7. *LEFT*: wire group efficiency; *RIGHT*: strip efficiency. This is a typical chamber.

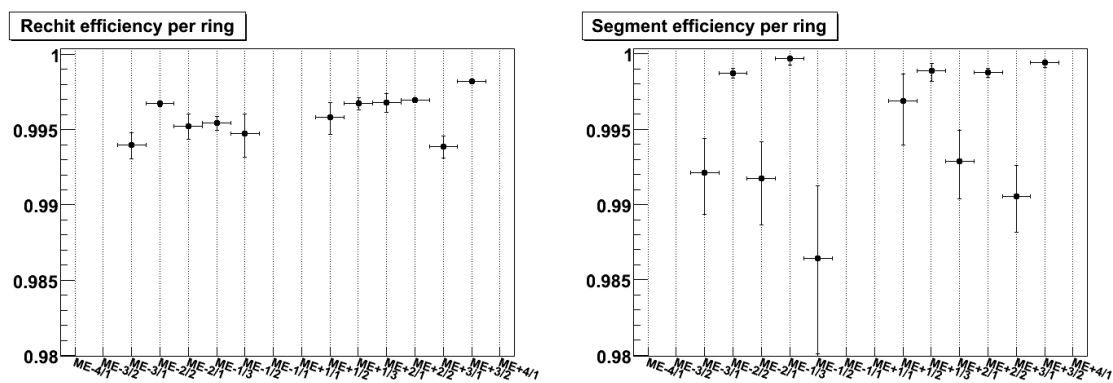


Figure 13: summaries of rechit and segment efficiencies, analogous to Fig. 10

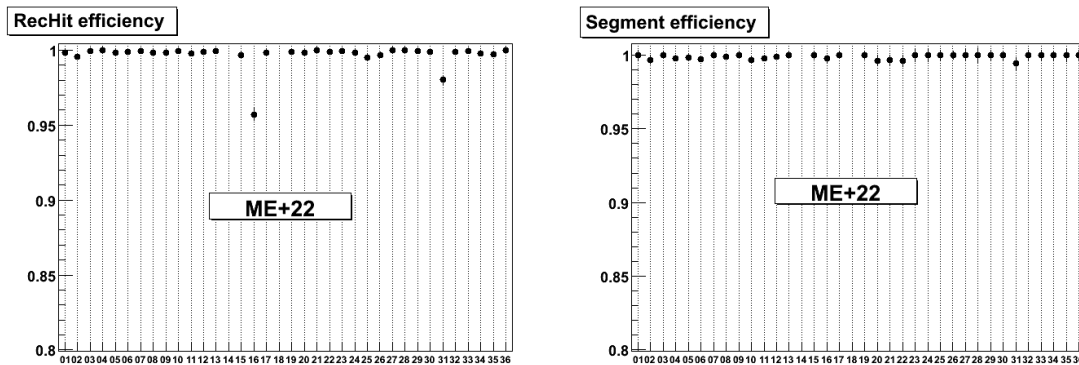


Figure 14: summaries of reconstruction efficiencies for all chambers in ME+2/2. *LEFT*: rechits, *RIGHT*: segments

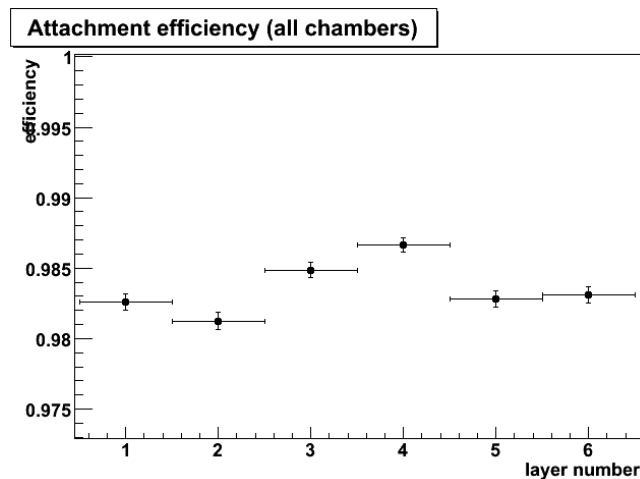


Figure 15: attachment efficiency for each layer

280 rechits used to build segments. It does not find segments in chambers with very many hits,
 281 due to prohibitive combinatorial problems – this will register as an inefficiency in the present
 282 study.

283 The segment efficiency for all the rings in the CSC system is shown in Fig.13, and specifically
 284 for the ME+2/2 chambers in Fig. 14.

285 3.6 Attachment Efficiency

286 The attachment efficiency is a characteristic of the segment finder. It is defined as the proba-
 287 bility of the segment to use a rechit from a given layer if there are rechits in that layer. As the
 288 segment finder could reject some rechits if their quality were poor, or if they were producing
 289 a bad fit, a very high value of the attachment efficiency is not the ultimate goal. What is
 290 important is that this efficiency should be reasonably flat as a function of the layer number.
 291 Any significant variation with layer number would be a hint of a problem – for example,
 292 an unacceptable dependence on the track angle. Fig. 15 shows that there is no bias in the
 293 CRAFT data.

294 4 Conclusions

295 The CRAFT data sample from 2008 allows detailed studies of efficiencies of the CSC subde-
 296 tector system. The offline analysis package `CSCEfficiency` has been developed to obtain
 297 accurate measurements of LCT, digi, rechit and segment efficiencies. In the course of these
 298 studies, a feature of the trigger peculiar to cosmic rays sometimes caused the track from a
 299 single cosmic ray event to be split between two events; changes to trigger timing have been
 300 made for the sake of cosmic ray running in 2009.

301 On the basis of the analysis presented here, the ALCT efficiencies are found to be well above
 302 99%, the strip, wire group and rechit efficiencies above 99.5%, the segment efficiency is
 303 at above 99%. The overall picture is consistent with previous measurements from MTCC
 304 data[7].

305 Acknowledgments

306 Many discussions with Ingo Bloch, Andy Kubik and Tim Cox were important to the devel-
 307 opment of this analysis. Ta-Yung Lin, Andrey Korytov and Khristian Kotov helped a lot to
 308 elucidate the split event problem.

309 Appendix A

310 This appendix lists the details of the configurable input parameters. These parameters should
 311 be moved to a python script (`cfi`) file; at present the defaults are set in the source file.

312 Configurable input parameters

```

313 printout_NEvents = pset.getUntrackedParameter < uint > ("printout_NEvents", 0);
    rootFileName = pset.getUntrackedParameter< string >("rootFileName", "cscHists.root");
    isData = pset.getUntrackedParameter< bool >("runOnData", true);
    isIPdata = pset.getUntrackedParameter< bool >("IPdata", false);
    isBeamdata = pset.getUntrackedParameter< bool >("Beamdata", false);
    getAbsoluteEfficiency = pset.getUntrackedParameter< bool >("getAbsoluteEfficiency", true);
    useDigis = pset.getUntrackedParameter< bool >("useDigis", true);
    distanceFromDeadZone = pset.getUntrackedParameter< double >("distanceFromDeadZone", 10.);
    minP = pset.getUntrackedParameter< double >("minP", 20.);
    maxP = pset.getUntrackedParameter< double >("maxP", 100.);
    maxNormChi2 = pset.getUntrackedParameter< double >("maxNormChi2", 3.);
    minTrackHits = pset.getUntrackedParameter< uint >("minTrackHits", 10);
    useTrigger = pset.getUntrackedParameter< bool >("useTrigger", false);
  
```

315 The following parameters have no default values. They need to be specified in the `cmsRun`
 316 configuration file.

```

hlTriggerResults_ = pset.getParameter< edm :: InputTag > ("HLTriggerResults");
[(HLTriggerResults = cms.InputTag("TriggerResults','HLT' ]
myTriggers = pset.getParameter< std :: vector<std::string>>("myTriggers");
[myTriggers = cms.vstring("HLT.L1MuOpen")]
andOr = pset.getUntrackedParameter< bool >("andOr");
[andOr = cms.untracked.bool(False)]
alctDigiTag_ = pset.getParameter< edm :: InputTag >("alctDigiTag") ;
clctDigiTag_ = pset.getParameter< edm :: InputTag >("clctDigiTag") ;
corrlctDigiTag_ = pset.getParameter< edm :: InputTag >("corrlctDigiTag") ;
stripDigiTag_ = pset.getParameter< edm :: InputTag >("stripDigiTag") ;
wireDigiTag_ = pset.getParameter< edm :: InputTag >("wireDigiTag") ;
317 rechitDigiTag_ = pset.getParameter< edm :: InputTag >("rechitDigiTag") ;
segmentDigiTag_ = pset.getParameter< edm :: InputTag >("segmentDigiTag") ;
simHitTag = pset.getParameter< edm :: InputTag >("simHitTag") ;
[alctDigiTag = cms.InputTag("muonCSCDigis","MuonCSCALCTDigi"),
clctDigiTag = cms.InputTag("muonCSCDigis","MuonCSCCLCTDigi"),
corrlctDigiTag = cms.InputTag("muonCSCDigis","MuonCSCCorrelatedLCTDigi"),
stripDigiTag = cms.InputTag("muonCSCDigis","MuonCSCStripDigi"),
wireDigiTag = cms.InputTag("muonCSCDigis","MuonCSCWireDigi"),
rechitDigiTag = cms.InputTag("csc2DRecHits"),
segmentDigiTag = cms.InputTag("cscSegments"),
simHitTag = cms.InputTag("g4SimHits", "MuonCSCHits")]
tracksTag = pset.getParameter< edm :: InputTag >("tracksTag") ;
318 [tracksTag = cms.InputTag("cosmicMuons")]

```

319 Next parameters will be part of the configuration in near future:

```

applyIPangleCuts = pset.getUntrackedParameter< bool >("applyIPangleCuts", false);
320 local_DY_DZ_Max = pset.getUntrackedParameter< double >("local_DY_DZ_Max", -0.1);
local_DY_DZ_Min = pset.getUntrackedParameter< double >("local_DY_DZ_Min", -0.8);
321 local_DX_DZ_Max = pset.getUntrackedParameter< double >("local_DX_DZ_Max", 0.2);

```

322 Discussion:

- 323 • `printout_NEvents` is used for printing general information in first specified
324 number of events (default is 0 events - no printout).
- 325 • `rootFileName` is the name of the output file containing the histograms.
- 326 • `isData` specifies the kind of input to be expected. If "false" the input is supposed
327 to be MC and thus specific MC (simulation) information is being accessed.
- 328 • `useDigis` is another condition regarding the input - if "false" then no access to
329 digis (LCT, strip, wire) is attempted and no efficiencies are calculated for them.
- 330 • `isIPdata` and `isBeamdata` further specify the input file(s) - collision (IP) data
331 impose "standard" processing. In case it is "false" the chambers under investi-
332 gation should be in the middle of the track. If both of the parameters are "false"
333 then Cosmic data is assumed. Beam halo and cosmic rays require special han-
334 dling of the direction of the propagation of the track - it is properly set by these
335 parameters.
- 336 • `getAbsoluteEfficiency` - if it is "false" then additional requirement is im-
337 posed for each investigated chamber - a minimum of 2 layers with rechit(s) is
338 required. This effectively removes "empty" (possibly dead) chambers from con-
339 sideration.

- 340 • `distanceFromDeadZone` is the cut imposed on the distance between the track
341 (propagation point) and the nearest dead zone of a chamber (including edges).
342 Track outside are not used for efficiency studies.
- 343 • `minP` and `maxP` are the minimum and maximum momenta required for the track
344 to be accepted as a probe whereas `maxNormChi2` and `minTrackHits` are the
345 maximum normalized chi2 and the minimum number of hits in the track allowed
346 for declaring the track a valid probe.
- 347 • `useTrigger` tells the program if the trigger selection is to me made - if it is "false"
348 no trigger is applied. If "true" - `myTriggers` tells which triggers are to be used
349 and in which condition (" andOr' ' - "true" denotes OR condition). It could be
350 given just one trigger name. The kind of triggers to be looked for are set by the
351 parameter in
- 352 • `hlTriggerResults_` (not necessarily HLT triggers). Then all the digi tags spec-
353 ify the proper names of the collection to be used. The same for the `simHit` tag.
- 354 • `tracksTag` specifies what kind of tracks are to be used as probe for the efficiency
355 measurements. The choice is important and influences many of the other param-
356 eters to be chosen.
- 357 • `applyIPangleCuts` is intended for use with non-IP data. If "true" -local angle
358 restriction on the propagated direction are applied for each investigated chamber.
359 The defaults of `local_DY_DZ_Max` (maximum allowed local direction dy/dz with
360 pointing from the IP),
- 361 • `local_DY_DZ_Min` and `local_DX_DZ_Max` are IP constraining and satisfy all the
362 stations and rings (not optimized but effective). The cut on dx/dz is on its absolute
363 value.

364 Appendix B

365 The `CSCEfficiency` package produces summary plots displaying the efficiency values in
366 per cent for all chambers. A so-called "temperature plot" is used, scaled so that 100% efficient
367 chambers are red. The chamber number is placed on the horizontal axis, and the ring number
368 is placed on the vertical axis. The statistical uncertainty is printed inside each box.

369 Fig. 16 shows the results for ALCT and CLCT efficiencies. Fig. 17 shows the results for wire
370 group and strip digis. Fig. 18 shows the results for rechit and segment efficiencies.

371 References

- 372 [1] CMS Collaboration, *CMS Physics Technical Design Report*, CERN/LHCC 2006-001 (2006)
- 373 [2] CMS Collaboration, *Studies of Muon Reconstruction Performance with Cosmic Rays*, CMS
374 PAPER CFT-09-014, *in preparation*
- 375 [3] J. Hauser et al., *Experience with Trigger Electronics for the CSC System of CMS*, Proceedings
376 of the 10th Workshop on Electronics for LHC Experiments and Future Experiments (2004)
- 377 [4] V. Barashko et al., *Fast algorithm for track segment and hit reconstruction in the CMS Cathode
378 Strip Chambers*, CMS NOTE-2007/023 (2007)

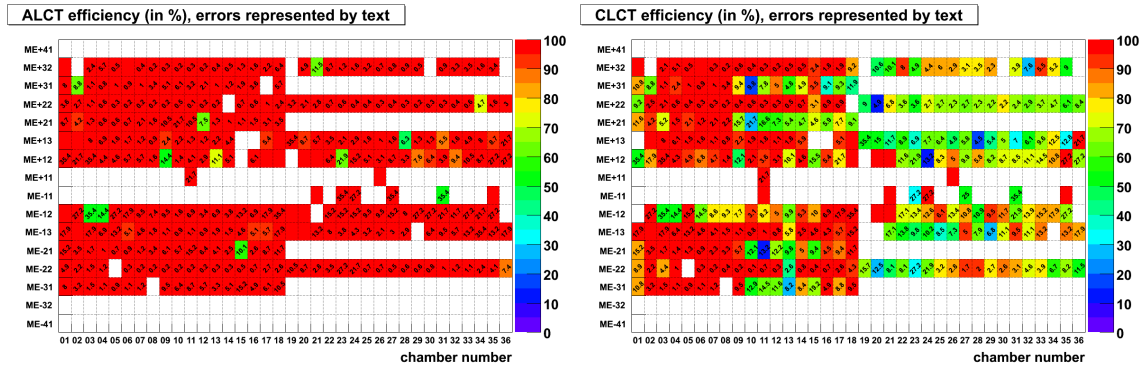


Figure 16: summary of ALCT (left) and CLCT (right) efficiencies for all chambers. The numbers in the boxes give the statistical uncertainty. Some chambers were not operational, and others could not be probed as they lie at the endpoints of stand-alone muon tracks.

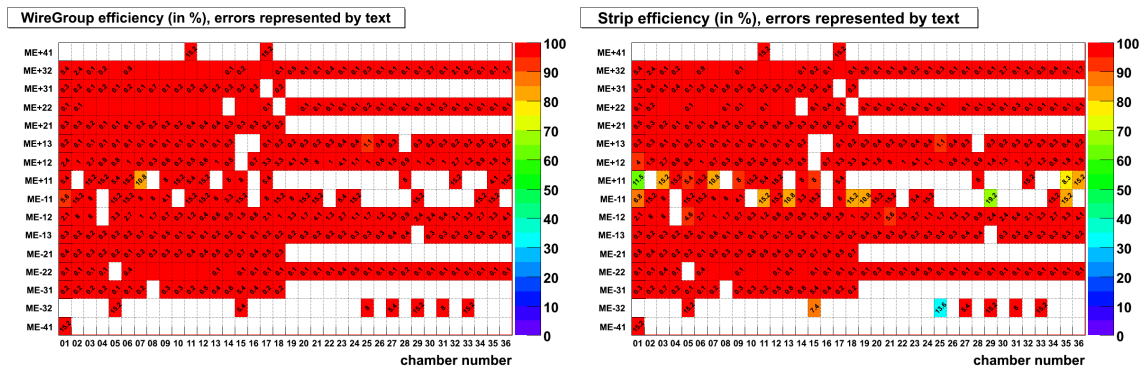


Figure 17: summary of wire group and strip digi efficiencies, analogous to Fig. 16

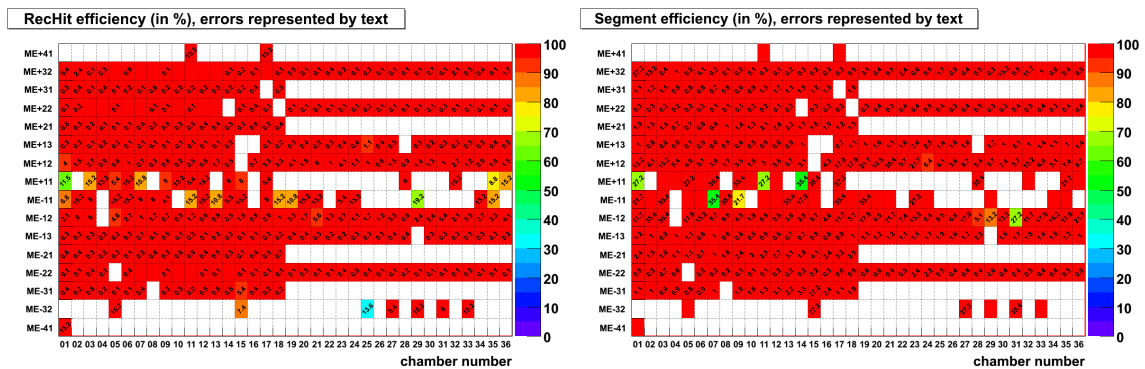


Figure 18: summary of rechit and segment efficiencies, analogous to Fig. 16

- 379 [5] W.-M. Yao et al., *Journal of Physics* **G33** 1 (2006)
- 380 [6] V. Barashko et al., *Fast Algorithm for Track Segment and Hit Reconstruction in the CMS Cath-*
381 *ode Strip Chambers*, *Nucl. Instrum. Meth.* **A589/3** (2008) 26 [CMS Note 2007/023]
- 382 [7] D. Acosta et al., *Measuring Muon Reconstruction Efficiency from Data*, CMS NOTE-
383 2006/060 (2006)
- 384 R. Breedon et al., *Efficiency of Finding Muon Track Trigger Primitives in CMS Cathode Strip*
385 *Chambers*, *Nucl. Instrum. Meth.* **A592** (2008) 26 [CMS Note 2007/031]